Simulation of Textile Stains

Yi Zheng, Yanyun Chen, Guangzheng Fei, Julie Dorsey, and Enhua Wu, *Member, IEEE*

Abstract—Modeling virtual textiles has long been an appealing topic in computer graphics. To date, considerable effort has been devoted to their distinctive appearance and physically-based simulation. The apperance of staining patterns, commonly seen on textiles, has received comparatively little attention. This paper introduces techniques for simulating staining effects on fabric. Based on the microstructure of yarn, we propose a triple-layer model (TLM) to handle the liquid-yarn interaction for the wetting and wicking computation, and we formalize the liquid spreading in woven cloth into two typical actions, the in-yarn diffusion and the cross-yarn diffusion. The dye diffusion is driven by the liquid diffusion and the concentration distribution of pigments. The warp-weft anisotropy is handled by simulation of the yarn's structure in the two directions. Experimental results demonstrate that a wide range of fabric stain phenomenon on different textile materials, such as the water ring effect, the high saturate stain contour, and the dynamic wash away effect, can be simulated effectively without loss of visual realism. The realism of our simulation results is comparable to effects shown in photographs of real-world examples.

Index Terms—Fabric appearance, capillary action, simulation, texture

✦

1 INTRODUCTION

TEXTILE stains are commonplace in our everyday experience and important for the realism of virtual clothes. Although various studies have been made on cloth modeling, deformation simulation, and rendering in the computer graphics literature, little attention has been paid to the simulation of stains. However, stains on fabric, like blood or mud, are essential to reinforce the visual realism in many applications, such as video games and movies. Without a practical simulation technique, artists must employ hand painting or use real-world pictures. Synthesizing the time-varying staining process with manual painting is labor intensive.

Staining is a complex process which involves various interactions occurring in the liquid-fiber interfacez, as well as pigment behaviors in the liquid and pigment interaction with yarn fibers. The distribution of yarn fibers in microscale significantly affects the wicking. The weaving style also has an impact on the stain appearance. Although staining is caused by the capillary action of liquid, direct application of the physical theory is not practical.

In this paper, we introduce techniques for the simulation of distinct textile stains. Our technique is based on a triple-layer model (TLM) which is specifically proposed for emulating the true nature of the staining behavior. In the TLM, the yarn-crossing model is then proposed as the basic computation structure for the simulation.

In our simulation, the staining process is decoupled into two phases, liquid diffusion and dye diffusion. Liquid diffusion is driven by the capillary pressure of yarns while dye diffusion is driven by the diffusion of liquid and the concentration of dye in the liquid. Specifically, the liquid diffusion phase includes two typical actions, the in-yarn diffusion, and the cross-yarn diffusion. The dye diffusion phase also covers two behaviors, the liquid-driven dye diffusion, and the concentration-driven diffusion This solution greatly simplifies the complex staining process for practical simulation and also handles the sophisticated stain effects such as dye accumulating on the contour, water ring around stains, and stain washed away.

The main contribution of the paper is to make the simulation of a wide range of textile stain practical in computer graphics. Specifically, the contribution includes the following aspects:

- A complete framework to simulate various stain effects on woven cloth;
- A triple-layer yarn model to simulate liquid interaction with yarns;
- A warp-weft anisotropy effect through yarn's structure simulation;
- A practical solution for cross-yarn liquid diffusion simulation.

2 RELATED WORK

Visual simulation of time-varying textile stains involves insights from a diverse range of research areas, including the basic physical theory, textile science, chemistry, and

- *Y. Zheng and Y. Chen are with the State Key Laboratory of CS, Institute of Software, Chinese Academy of Sciences, Beijing 100864, China, and the University of Chinese Academy of Sciences, Beijing 100190, China. E-mail: zhengyi7592@sina.com, chenyy@ios.ac.cn.*
- *G. Fei is with School of Animation and Digital Arts, Communication University of China, Beijing 100024, China. E-mail: gzfei@cuc.edu.cn.*
- *J. Dorsey is with Yale University, New Haven, CT 06520. E-mail: julie.dorsey@yale.edu.*
- *E. Wu is with the State Key Laboratory of CS, Institute of Software, Chinese Academy of Sciences, Beijing 100864, China, the University of Chinese, Academy of Sciences, Beijing 100190, China, the University of Macau, Taipa, Macau 999078, China, and also with the Zhuhai-UM Science and Technology Research Institute, Zhuhai 519080, China. E-mail: ehwu@umac.mo.*

computer graphics. Here, we briefly survey the most relevant work in these various domains.

Physics and Textile Science. The surface tension of liquid plays the most critical role in capillary action, the inner drive for forming textile stains. Theory of capillary action can be found in textbooks and journals such as [1], [2], [3]. Washburn's equation predicts the movement of liquid in an ideal capillary tube [4] and Wiener [5] defines a thread as a formation of sufficient length, with a circular cross-section, in a constant filling, but without any variation in linear mass of the thread. In textile science research has focused on the wicking and wetting of textile materials [5], [6], [7], [8], [9]. Patnaik et al. [8] pays more attention to fibrous materials while Zhang et al. [9] proposed an equilibrium model for spontaneous liquid wicking into the longitudinal textile from an infinite liquid reservoir. Zhu [10] studied the liquid flow in fabric based on the principle of the capillary action, Lukas and Glazyrina [11] simulated the wetting of fiber using the Ising model, Huber et al. [12] used a simple adhesion model to simulate the stickiness of wet clothes, Mhetre and Parachute [13] explored the yarn-to-yarn liquid migration, Liu et al. [14] investigated vertical wicking in twisted yarns and Mhetre [15] measured the relationship between different textile materials and a given liquid.

Physically-Based Wet Clothes Simulation. Physically-based simulation of dynamic clothing is one of the most active areas of research in computer graphics today. Basori et al. [16] and cited references give an excellent overview on deformation simulation of clothes in computer graphics. Of note, simulating the deformation of wet clothes is in itself an active research area and several studies [17], [18], [19]. focus on the changes of clothing geometries caused by external or internal forces.

Wet and Time-Varying Appearance. There have been a few studies on the simulation of textile stains in the computer graphics literature. Dorsey et al. [20] provides a comprehensive description of modeling advanced materials including textiles and fur. One of the most relevant models was proposed by Jensen et al. [21] which focuses on the rendering of wet materials. Dorsey et al. [22] used Darcy's law simulation of fluid flowing through a porous medium to capture the appearance of stone. Lu et al. [23] synthesized the drying phenomena. Chu et al. [24] introduced a physically-based method for simulating ink dispersion in absorbent paper and Gu et al. [25] and Lu et al. [26] proposed techniques to measure, represent and render time-varying surface appearance. Two 2007 papers [27], [28] employed Fick's second law and the woven fabric's structure to simulate the dyeing effect. Some typical models of adsorption isotherms are well adopted to simplify the operations. Lenaerts et al. [29] combined Darcy's Law and the Smoothed Particle Hydrodynamic (SPH) technique to simulate fluid flowing through a deformable porous material.

Computer Generated Painting. There are many computer generated painting papers that are related to our work. Curtis et al. [30] introduced a technique to create the watercolor effect by employing a three-layer fluid model for simulating the flow of water above paper. In their approach, the adsorption and desorption of pigment and the transport of water through pores are similar to the liquid transport in the fabric bundle of yarn. Chu et al. [24] presented a physically-based method for simulating ink dispersion in absorbent paper, where the lattice Boltzmann equation was used to simulate water percolation and hydrodynamic dispersion was employed to model the pigment advection. However, these techniques cannot be applied to the simulation of stains since they have not taken into consideration the structure of woven cloth as well as the special microstructure of yarn. This is also the case with other works by Xu et al. and Wang [31], [32].

Textile Appearance. The appearance of textile materials has been an attractive topic for more than a decade. Adabala et al. [33] introduced techniques for visualizing woven clothes in real time and Daubert et al. [34] presented BTF-like techniques to render fabrics based on replicating weaving or knitting patterns. Earlier works include Groller et al. [35] who used a volumetric representation for knitwear rendering and Xu et al. [36] who proposed a special structure named *lumislice* to model and render knitwear realistically. Recently, Jakob et al. [37] introduced anisotropic scattering by which a radiative transfer framework was proposed to capture the appearance of volumetric objects including textile materials. Zhao et al. [38] synthesized volume data of fabric using micro CT imaging. However, all the works above focused on clean fabric material without consideration of stain. Morimoto et al. [28] employed Fick's second law and the woven fabric's structure to simulate and visualize the dyeing effects. Some typical models of adsorption isotherms are well adopted to simplify this process. The focus of our work, however, is to make visual simulations of general staining effects for gaming and other computer graphics applications. Therefore, we introduce an abstract model TLM to simplify the physical process and generate various staining effects, such as the detail of irregular stain shapes, the accumulation of pigment at the stain boundaries, and the appearance of water-ring effect during the simulation, which will eventually vanish by evaporation.

3   LIQUID DIFFUSION

When liquid contacts with a fabric surface, it will be absorbed and spread if the fabric is wettable. This liquid diffusion process is involved with wetting and wicking, and as a consequence, a stain pattern will be eventually generated on the fabric surface.

Physically, liquid diffusion into fabric is mainly driven by the capillary force, which governs how liquid moves and is held in a thin tube. Dye pigments as staining material either dissolve in liquid or are suspended in the liquid following the moving behavior of liquid advection and diffusion, both of which produce a color change in the liquid. However when the liquid is running through the micro-tube in the fabric fibers, dye pigments attach to the fiber surface by chemical bond or are blocked by the microstructure This relates to the colorfastness of the fibers to the given dye (colorfastness is the relative value; different dye pigments have different values with the same fabric material).

For woven textile, liquid-yarn interaction is essential for simulation computation. Liquid-yarn interaction depends on the organization of fibers which form the yarn and the hydrophobicity of the fiber material. For practical simulation, a triple-layer yarn model is proposed to formalize the structure of yarns.
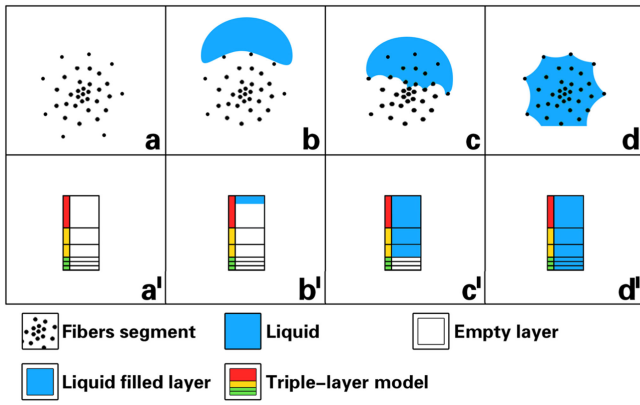
Fig. 1. The TLM and the wetting process. The liquid penetrates the fibrous layer and wicks into the fibre bundle.

3.1 Triple-Layer Model

In textile research, a yarn can be regarded as a bundle of fibers [5] coated with a fibrous layer [8] because these interlocked fibers are packed closely inside and loosely outside. The liquid absorbed by the yarn's capillary action from outer to inner requires a progressive transition procedure. Although different yarns may look similar, different fibers give them distinct properties when interacting with liquid. Usually, these fibers are divided into two types, natural fibers, and synthetic fibers. The structure of natural fibers is far shorter and looser than synthetic ones. As a result, natural yarns have more capillary tubes and larger inner space for liquid transportation. To make the simulation practical, a triple-layer model TLM is proposed. The tight inner fiber bundles act as a transport-layer, the loose outer fiber bundles as an occlusion-layer, and the outer fibers as a transition-layer, as shown in red in Fig. 2. The thickness of transport-layer, occlusion-layer and transition-layer is denoted as d_0, d_1 and d_2 respectively. Note that some synthetic mixed fabrics can have very thick transition-layer ($1 \gg d_2 > 0$) while some other fabrics like pure polyesters may have no transition-layer at all ($d_2 = 0$).
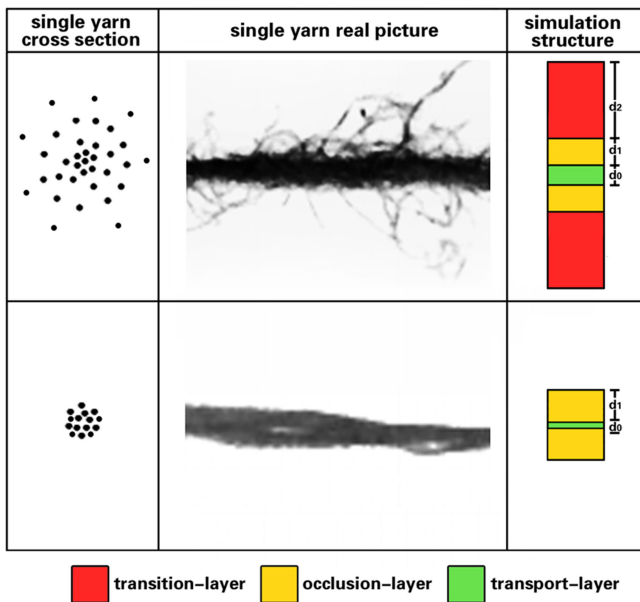

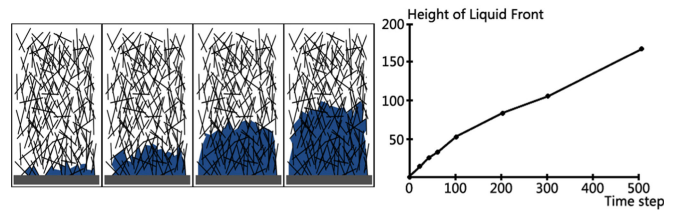Fig. 2. The real pictures of yarns and the TLM.

Fig. 3. The wetting computed using the Ising model.[D. Lukas 1997].

3.2 Wetting

The images at the top row of Fig. 1 show the whole wetting process of a yarn. When liquid touches a yarn, the air pockets created by the fibers in the transition-layer are trapped underneath. Image **b** in Fig. 1 shows this state. The wetting here is the process of the liquid exchange with the air pockets and gradual diffusion from the transition-layer to the transport-layer. Image **c** in Fig. 1 shows this intermediate state. When the liquid front reaches the transport-layer, the liquid is quickly transported driven by the capillary pressure, and the wetting is completed. The bottom row of the images shows the simulation of this process using the TLM. Fig. 3. Lukas et al. [11] shows the detail of this process in microscale.

The computation of this wetting process can be very complex because it depends on the hydrophobicity of yarn fiber and the microstructure of the yarn's fiber mass which is very hard to model. In the textile study, the Ising model has been used for this computation [8], [11] such as in Lukas et al. [11] where the authors employed a Monte Carlo technique to make the simulation of the wetting behavior of fibrous materials. The most interesting part of this work is the height of the liquid front which turns out to be nearly proportional to the wetting time. In other words, the wetting here can be loosely defined as a linear process. Practically we define an abstract parameter, the wetting computation thickness for $d_1 + d_2$. The wetting process is thus simplified as $F(n + 1) = F(n) + \Delta F$. Here $F(n)$ is the liquid front. ΔF is the marching size of each time step which can be simplified using a constant value since the wetting progress is almost linear. The wetting process is then ended at $F(n) = d_1 + d_2$. So the larger the value of $d_1 + d_2$, the longer the wetting time. The wetting process can occur from outer to inner layers, or from inner to outer, and that process affects liquid cross-yarn diffusion.

3.3 Liquid Transport in Yarn

After wetting, the staining liquid penetrates the transition-layer and spread to the transport-layer. We term the spreading of liquid along the yarn as in-yarn diffusion. The main factors affecting in-yarn diffusion include the liquid free movement in-yarn segment and the liquid movement driven by the force from the capillary pressure gradient. The maximum amount of liquid a yarn segment can hold is determined by [15]

$$W_h = \frac{\rho_l(\phi)}{\rho_s(1 - \phi)},$$

where W_h denotes maximum liquid held in a yarn segment, ρ_l is the liquid density, ρ_s is the density of the fiber, and ϕ is the fabric porosity (the values of ρ_l, ρ_s and ϕ could be obtained from Textile Sciences LUT). When liquid passes through yarns, some liquid stays. A certain amount of
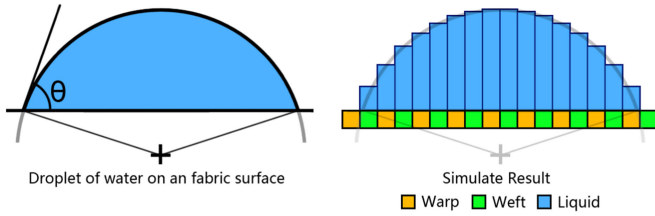
Fig. 4. The contact angle and the discrete representation of a liquid drop for the simulation.

Fig. 6. Cross-yarn liquid transport. The upper row shows the liquid transport process in natural yarn ($d_2 > 0$). The lower row shows the liquid transport process in synthetic yarn ($d_2 = 0$).

liquid, $\epsilon(\epsilon < W_h)$, is trapped at any wetting locations because of the fiber hydrophilicity (ϵ is decided by the fiber's structure and material). That means if the liquid volume in the yarn segment is larger than ϵ, liquid diffusion could happen. This is caused by the differential of local capillary pressure, P, which comes from the liquid surface tension, and can be expressed by

$$P = 2\gamma \, cos \, \theta \, /r, \tag{1}$$

where γ is the liquid surface tension, r is the internal radius of the yarn fiber tube, and θ is the contact angle, the angle at which the liquid-vapor interface meets the ideal solid-liquid interface, as seen in Fig. 4 (θ value could be obtained by the contact angle measurement method). Capillary pressure appears when a yarn segment is wet but unsaturated. Liquid in a yarn flows from lower capillary pressure regions to higher ones. The flow rate Φ is calculated by Poiseuille's Law

$$\Phi = \frac{\Delta P}{R_f} = \frac{\Delta P}{8\eta L/(\pi r^4)} = \frac{\pi r^4 \Delta P}{8\eta L}. \tag{2}$$

Here L is the length of the tube, η is the dynamic fluid viscosity. r is the radius of tube radius. ΔP is the pressure difference between the start and end points of the tube. The capillary pressures of consequent yarn segments are calculated by the discrepancy of the liquid saturation. For example, when a yarn segment Y_1 at 60 percent saturation connects to a yarn segment Y_2 in 40 percent saturation, the pressure difference between them is $(60\% - 40\%) \times P$. Here P is the maximum capillary pressure of Y_2 calculated by Equ. (1).

3.4   Liquid Transport in Woven Textile

With the knowledge of liquid-yarn interaction, we can now study the stain liquid transport in a woven cloth. Here a basic computation unit, the yarn-cross is proposed for the simulation.

3.4.1   Yarn-Cross

Woven cloth is created by the warp and weft yarns. The cross of a warp yarn segment and a weft one create the basic
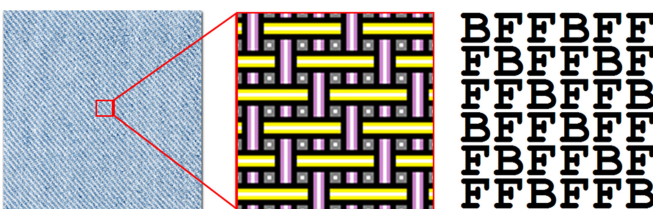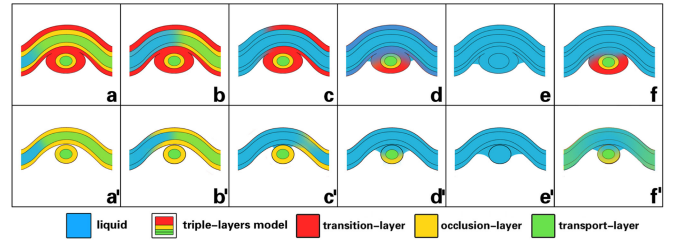

Fig. 5. A twill fabric represented by yarn-crosses. Left to right: the twill fabric, the weaving structure, and the yarn-cross orientations (F for front facing and B for back).

unit of most woven textiles. Fig. 5 shows a twill fabric and the distribution of the yarn-cross.

3.4.2   Cross-Yarn Diffusion

As was pointed out by Zhu et al. [10], when the liquid flow front of a warp yarn encounters a weft yarn, some liquid in the warp yarn may move into the weft one, or vice versa. We call this liquid transmission cross-yarn diffusion as shown in Fig. 6.

Similarly, the cross-yarn diffusion is dominated by the capillary pressure differential. Natural yarn ($d_2 > 0$) and synthetic yarn ($d_2 = 0$) are quite different when the cross-yarn diffusion is being performed.

Cross-Yarn Diffusion of Nature Fabric. For natural yarns, the structure at the intersection position has a little change; because two yarns press each other, the space between yarns is filled up by the fibers. As a result, the transition-layer which coats the yarn's surface mixes together as shown (image **a**) in Fig. 6.

When the liquid front in the weft yarn reaches the cross-yarn position, the occlusion-layer and transition-layer are not wetted because the liquid in the tight-fibers tube (transport-layer) always moves faster (image **b**). The liquid front moves on and the wetting process from inner to outer proceeds (image **c**). Next, the occlusion-layer and transition-layer are wetted, the liquid transition channel has thus been built up, and cross-yarn transition starts (image **d**). The amount of liquid that is transferred depends on the differential of the capillary pressure of the two yarns.

Image **e** shows that if the liquid volume in yarn segment is over the yarn's maximum water volume (W_h), water would flow over the yarn's surface as the yarn is oversaturated.

Image **f** shows that if the liquid volume in yarn segment is far less than the yarn's maximum water volume (W_h) due to the existence of the transition-layer, the liquid could be held in the sub-micro space built up by the fibers, so the liquid transition channel would be maintained until the liquid evaporated.

The wetting step for cross-yarn liquid transmission is very important because for some material like wool, the wetting step can take an extended period and therefore the in-yarn diffusion dominates the liquid spreading. Images in Fig. 11 shows this distinctive effect.

Cross-Yarn Diffusion of Synthetic Fabric. For synthetic materials like polyester, there is no evident transition layer, therefore, no outer wetting. However, they also require connections for cross-yarn liquid transmission. Migration of liquid from one yarn to another occurs only when the yarn becomes sufficiently saturated so that the liquid available on

the surface of the yarn may form a tiny reservoir located at the gap between the two yarns. Unlike the natural yarns, this connection is not stable and breaks once the reservoir vanishes.

Images at the bottom of Fig. 6 show this process. Image **a'** shows the structure change at the intersection position of the yarns. Image **b'** shows the liquid wetting from the inner transport-layer to the outer occlusion-layer. When enough liquid passes through the connection area and the reservoir is already set up, the liquid connection is then created (image **c'** and **d'**).

When there is not enough liquid, the reservoir will shrink. Because the transport-layer capillary action is stronger than the capillary generated by the cross-yarn nodes' gap, and there is no transition-layer coat the yarn to maintain the transition channel, so the liquid transported is affected by the yarn's saturation and shown by the image **f'**.

By this, we can simulate the special staining effect on polyester as it distributes first on warp and weft respectively coming up like a cross, then a diamond, and eventually an ellipse.

3.4.3 Warp-Weft Anisotropic

Most of the stains on woven cloth appear as warp-weft anisotropic. This is a multifactorial effect. First, the weaving style creates different organization on warp and weft yarns and most fabrics have different densities of yarn on warp and weft directions. Second, the warp yarns and the weft yarns may not have the same twist. Twist of yarn is also an important factor that affects the capillary pressure and wicking speed [14]. Third, fiber tubes of the warp yarns and the weft yarns can have different radii. Equ. (2) shows that the radius is important for the liquid transmission.

Precisely calculating the warp-weft anisotropic is complex. As the anisotropy is caused by the discrepancy of the wicking speeds, it can be captured by giving different diffusion-coefficients, $f^{|}$ and f^{-}, to the warp and weft yarns. Liquids in higher diffusion-coefficient yarn go faster and therefore creates a larger stain. This ratio of the two coefficient, $f^{|}/f^{-}$, can be easily calculated by measuring the warp and weft size of a real stain.

3.4.4 Liquid Diffusion Connection

We sum up in the flowing algorithms on the cross-yarn liquid diffusion: the Equ. (3) below is applied to calculate the liquid cross-yarn diffusion volume L_c

$$L_c = \max(0, \Phi - \epsilon) \cdot \frac{P_c}{P_l + P_c} \cdot C. \tag{3}$$

Here Φ is the liquid volume through the yarn segment, ϵ is the liquid held in the yarn segment, P_c is the cross yarn diffusion probability, P_l is the in yarn diffusion probability, C is the connectivity between the warp and weft yarn in the node, with its range from 0 to 1, so C is the key parameter which affects the final liquid diffusion result.

C marks cross-yarn diffusion effect: if $C = 0$, cross-yarn diffusion is broken, otherwise, there is an in-yarn diffusion calculated by

$$C = min(1, \lfloor (d1^{|}_w + d1^{-}_w) \cdot 0.5 \rfloor \cdot \lfloor (d2^{|}_w + d2^{-}_w) \cdot 0.5 \rfloor). \tag{4}$$

Equ. (4) simulates the natural yarn's wetting effect ($d_2 > 0$). $d1^{|}_w$ and $d1^{-}_w$ are the yarn's occlusion-layer wetting process, $d2^{|}_w$ and $d2^{-}_w$ are the yarn's transition-layer wetting process, $\lfloor$ and $\rfloor$ show if the two yarn's do not finish the wetting step in that node, C is equal to 0 until wetting step completed.

$$C = min(1, \lfloor (d1^{|}_w + d1^{-}_w) \cdot 0.5 \rfloor \cdot S_w). \tag{5}$$

Equ. (5) simulates the artificial yarn's wetting effect ($d_2 = 0$). $d1^{|}_w$ and $d1^{-}_w$ are the yarn's occlusion-layer wetting process, S_w is the node's saturation, the equation shows that if the node's saturation is not overflow, C is equal to the liquid saturation in that node.

3.5 Evaporation

Liquid evaporation takes place when fabric is wet. It is simulated by reducing the amount of liquid in the fabric as it vaporizes into a gaseous phase. The evaporation influences the size, shape and saturation distribution of stains. The evaporation ratio is dependent on the environmental temperature and air contact area. To simplify the simulation, evaporation is regarded as a linear function that reduces a given amount of liquid, Δe in each iteration.

Evaporation ratio, Δe is very important for the stain simulation. Fig. 18 shows the impact of this coefficient.

4 DYE DIFFUSION

Dye spreads with liquid and eventually changes the color of the stained region on fabric. In our simulation, the dye diffusion consists of three processes: liquid-driven diffusion, concentration-driven diffusion, and the dyeing process.

4.1 Liquid-Driven Diffusion

The liquid-driven diffusion is the most important process for dye spreading in stains. The dye substances carried by the staining liquid are spread in the fabric by the in-yarn diffusion as well as the cross-yarn diffusion. Without considering the deposition of the dye particles, or the forming of chemical bonds between the ion and yarn fiber, the amount of dye substances spread by the liquid-driven diffusion process is proportional to the amount of staining liquid.

4.2 Concentration-Driven Diffusion

The concentration differential is mainly caused by evaporation. The concentration-driven diffusion tries to compensate for the uneven distribution of dye. Fick's second law predicts how the concentration of substance in liquid changes with time

$$\frac{\partial \phi}{\partial t} = k_d \frac{\partial^2 \phi}{\partial x^2}, \tag{6}$$

where ϕ is the concentration, t is time, x is the position, k_d is the diffusion coefficient, proportional to the squared velocity of the diffusing substance, which depends on the temperature, viscosity of the liquid and the size of the substance particles according to the Stokes-Einstein relation. In dilute aqueous solutions, the diffusion coefficients of most ions are similar and have values that at room temperature are in the range of 0.6×10^{-9} to $2 \times 10^{-9} \text{ m}^2/\text{s}$. For

TABLE 1
The Coefficients of Staining Simulation

	$d_0^{\vert}, d_0^{-}$	radius of the tight fibres tubes (transport-layer)
*	$d_1^{\vert}, d_1^{-}$	thickness of the loose fibres layer (occlusion-layer)
*	$d_2^{\vert}, d_2^{-}$	thickness of the fibrous layer (transition-layer)
*	$W_h^{\vert}, W_h^{-}$	maximum liquid held
*	$f^{\vert}, f^{-}$	diffusion-coefficient
*	ϵ	minimum liquid held of the fibres
*	$D_f.$	dye fastness
	D_s	dye saturation
	D_c	dye color
	Δe	evaporation ratio
	$d1_w^{\vert}, d1_w^{-}$	wetting progress of the occlusion-layer
	$d2_w^{\vert}, d2_w^{-}$	wetting progress of the transition-layer

*Means it is a local coefficient that need to specify for each yarn-cross, super-scripts $^{\vert}$ and $^{-}$ denote the warp and weft directions.

biological molecules the diffusion coefficients normally range from 10^{-11} to 10^{-10} m^2/s.

Compensation of concentration-diffusion diffusion is subtle. The liquid-driven diffusion dominates the transmission of dye substance. Considering the stain center as a reservoir that holds more liquid, the liquid diffusion keeps transferring liquid to the contour region because of the evaporation. Dye substances accumulate there and grow up to become a contour. This effect is evident in the artificial fabrics which have lower colorfastness. Images on the left of Fig. 11 show this effect.

4.3 Dyeing

Dyeing is driven by the capillary action between the stain liquids and the yarn fibers. The dyeing process that eventually forms the shapes and appearance of stains is affected by many factors, including the deposition of stain substance after liquid evaporation, stuck particles at the gaps of yarn fibers, and the formation of chemical bonds between yarn fibers and dye ions. The chemistry of stain dyeing can be very complex and involves many different kinds of liquids and staining substances as well as different dyeing processes. Dye ions or other chromatic pigments in the stain liquid can adhere to yarn fibers in different ways. Dye ions may stick to the fibers and create chemical bonds. Big particles may get stuck into fiber gaps and stop moving. Since our stains simulation focuses on the change of textile appearance, a simple coefficient, the colorfastness, D_f, can be specified to represent this effect. Note that D_f is related to not only the dye but also the fabric material. A lower D_f means that it is easier for the pigment to be carried away. Dye color saturation D_s is an interesting coefficient. Higher dye colorfastness D_f combined with lower color saturation D_s leads to the *water ring* effect, as is shown in Fig. 17. This is because the solution spreads faster than the dye. We also test the effect of the evaporation ratio Δe and the dye color saturation D_s. In Fig. 18 we simulate the stains on a polyester by the same amount of stain liquid using different Δe. The example clearly shows that the evaporation ratio affects not only the size but also the shape and dye saturation distribution of the stain.

5 IMPLEMENTATION

By the above technique, we can easily build the system for stain simulation. A woven fabric article is represented as a

TABLE 2
Some Key Values of the Simulations

material	d_0	d_1	d_2	ϵ	$W_h^{\vert}/W_h$	$f^{\vert}/f^{-}$	D_f
cotton	0.5	0.1	0.2	0.2	0.4/0.4	1.0/0.8	0.5
polyester	0.1	0.5	0.0	0.05	0.3/0.3	1.0/0.6	0.1
wool	0.5	0.5	1.0	0.3	0.8/0.8	1.0/0.9	0.5

2D matrix of yarn-cross $\mathbf{M}$, as is shown in Fig. 5. The basic idea is to calculate the capillary pressure differentials for the warp and weft yarn segments of each yarn-cross and then perform liquid transport by Equ. (2) iteratively. The capillary differentials are calculated on the network of connected yarn segments. This connectivity includes the nature connection of the yarns, and the dynamic liquid connection defined by C in Equ. (3). d_0, d_1, and d_2 can be measured using real yarns while W_h, f, D_f, ϵ, and Δe can be obtained from figures in textile textbooks. The efficiency of the proposed technique allows artists to fine tune these values for desirable results.

Table 1 lists the coefficients that are used for the simulation, and Table 2 provides the values of the coefficients that are used in our simulations.

5.1 Simulation Algorithm

After discretizing a textile material into yarn-cross $\mathbf{n}$ represented by matrix $\mathbf{M}$, the stain simulation could be made by the following algorithm:

Algorithm 1. The Main Iteration Loop
---
for Each warp and weft direction **do**
  for Each yarn node in $\mathbf{M}$ **do**
    calc. the local capillary pressure by Equ. (1);
    calc. the ΔP of liquid-connected yarn segments;
    UpdateLiquidConnectivity();
    LiquidDiffusion();
    DyeDiffusion();
    Do evaporation;
  end for
end for

The three subroutines, *UpdateLiquidConnectivity()*, *LiquidDiffusion()*, and *DyeDiffusion()*, are given by Algorithms 2, 3, and 4.

Algorithm 2. UpdateLiquidConnectivity()
---
if $d_1 > 0$ **then**
  do liquid wetting progress by simplified Ising model;
  update C by Equ. (4);
else
  update C by Equ. (5);
end if

Algorithm 3. LiquidDiffusion()
---
calculate in-yarn diffusion by Equ. (2)
if $C > 0$ **then**
  calculate cross-yarn diffusion by Equ. (3)
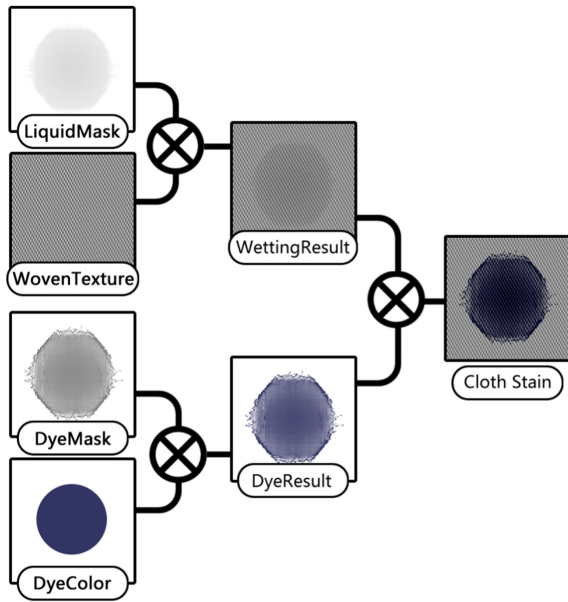**end if**

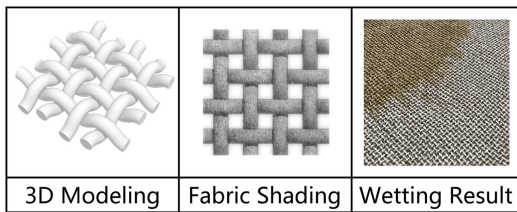Fig. 7. The render pipeline of stain visualization.

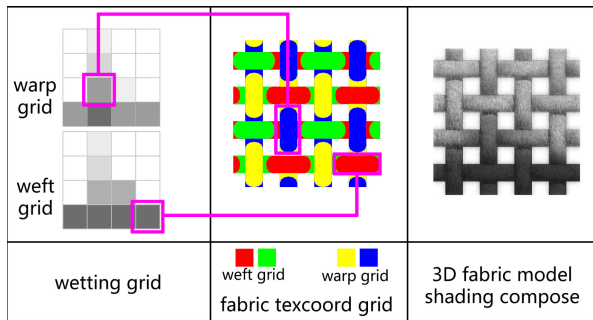Fig. 8. The virtual fabric rendering method.

Fig. 9. Composition of wetting effect with virtual fabric. The image on the left shows warp and weft wetting result, and in the middle shows how the wetting mask is aligned with fabric structure by the grid indices. The image on the right shows the composed effect.

Algorithm 4. DyeDiffusion()

calc. liquid-driven dye diffusion;
calc. concentration-driven diffusion by Equ. (6);
dye deposition;

To start the simulation, the given stain liquid is discretized into liquid columns and acts as water sources to the touched yarn-cross as the initialization condition, as shown by the right image in Fig. 4.

5.2 Stain Rendering

The results of liquid and dye distribution can be exported as degree masks for rendering at any simulation step. The liquid mask is used to modify the translucency of the fabric
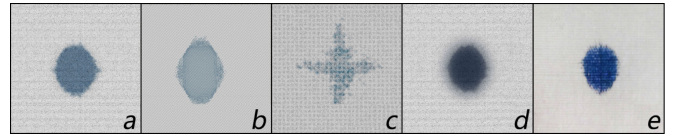

Fig. 10. Comparison of stains. The Images *a*, *b* and *c* are our results (*a* is cotton, *b* is polyester, *c* is wool), and the image *d* was generated by the technique published in the ref. [28]. The image *e* on the right is a real cotton fabric picture. By TLM, we could get more realistic wetting results on different fabric material.
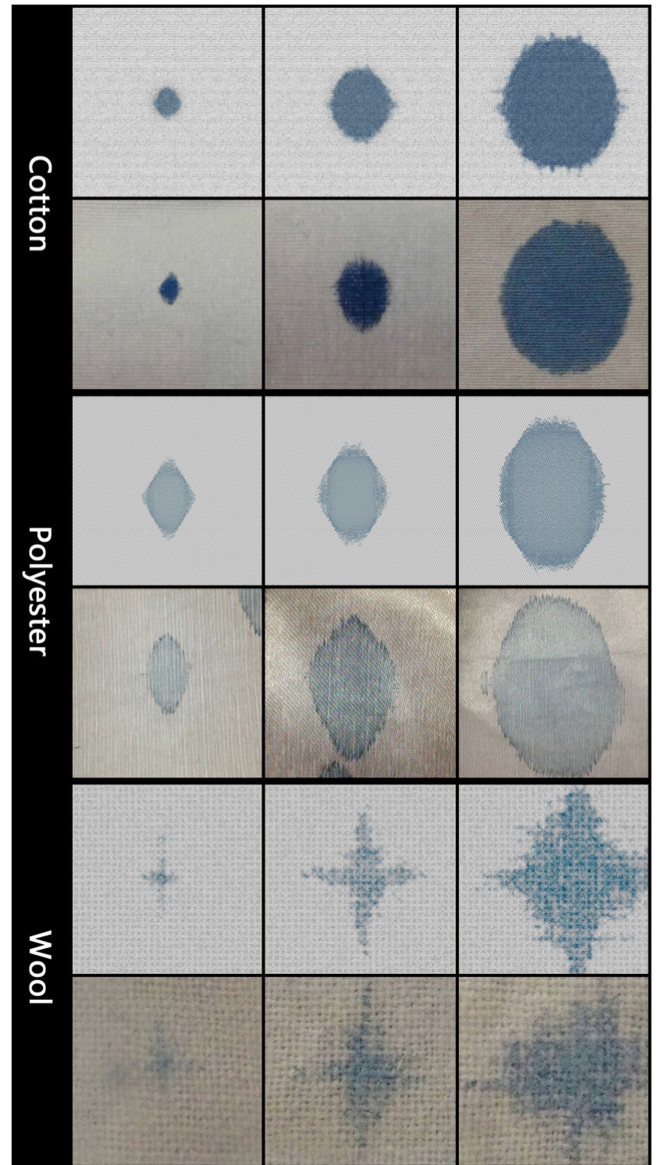

Fig. 11. Synthesis results (upper) versus real pictures (lower) in pair. From top to bottom: cotton, polyester, and wool. Liquid increases from left to right.

and its surface appearance, as [21] does. The dye mask with the given dye color is used to modify the intrinsic color of the yarns. Fig. 7 shows the two masks and the rendering process. The liquid mask with the woven texture is used to render a piece of wet fabric whose intrinsic color would be further modified by the local color of dye deposition synthesized from the dye mask and the given dye color. Fig. 8 shows virtual fabric modeling and rendering in three steps. The first step is 3D modeling the fabric's yarn structure and

Fig. 12. Stains of coffee on different fabrics: See the different on the edges.

Fig. 13. Motions of two dyes in different colors. The edge spreading starts in the middle image eventually forms a transitive region between the two colors in the right image.

Fig. 14. Stain of wine. Wine has low dye saturation therefore the water ring can be clearly observed during the simulation. The cotton tablecloth has high colorfastness that the dye has limited spreading.

rendering with Lambertian shading model. The second step is overlap fibrous effect generated by hair and fur rendering algorithm. The third step is the composition of fabric effect with liquid diffusion and dyeing masks effect; the masks modify the local fabric's BRDF. Fig. 9 shows how to compose wetting result with virtual fabric.

6 EXPERIMENTAL RESULTS

In this section, we show some experimental results of the proposed technique. The first one is a comparison with the technique proposed by Morimoto et al. [28]. Fig. 10 shows this comparison. The methods both in [28] and our TLM could simulate the stain effects convincingly on fabrics like cotton. However, our TLM can simulate patterns on a broader range of materials, such as wool and polyester.

To verify the proposed technique, the simulation results are compared with real pictures. In Fig. 11, three comparisons in pair are made on cotton, polyester, and wool respectively. In each pair, the synthesis result in upper image is compared with the real picture in lower one. The amount of

stain liquid increases from left to right. This figure shows that the simulation results of our system are comparable to the real pictures.

Some interesting effects can be observed from this figure. First, natural yarns like cotton (top) and wool (bottom) tend to have higher dye fastness D_f than synthetic yarns like polyester (middle). Therefore higher D_fs are given to cotton and wool that lead to the results whose saturation of the stain color distributes evenly in the stain. For polyester which has a lower D_f, the color pigments are driven by the movement of the liquid and accumulate to the contour of the stain.

Another effect is the setting of wetting computation thickness d. Wool yarns have a thinker fibrous-coat layer, therefore, have very high wetting cost. The in-yarn diffusion dominates the liquid spreading, therefore, the shape of the stains is irregular.

Next, we simulate stains in virtual scenes. Fig. 12 shows two coffee stains with zoom-in details. The same amount of coffee liquid on different fabrics results in stains of very different shapes. Fig. 13 shows the interaction of two stain
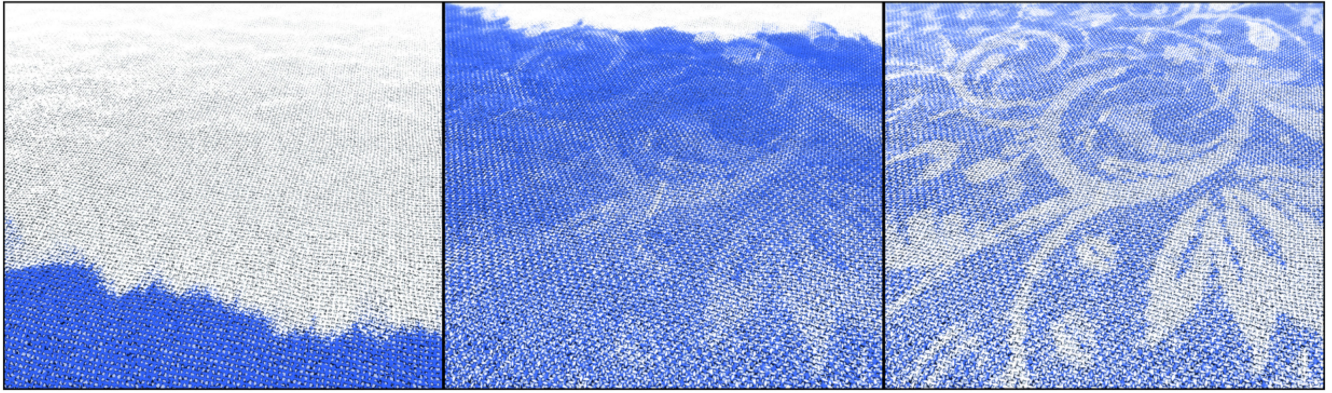
Fig. 15. Wax printing, a traditional dyeing process. First, artists paint flower pattern by wax on the fabric. Then, the fabric is washed using blue dye liquor many times. Finally, the color on the waxing area is washed away and the beautiful pattern appears.

Fig. 16. Wash away. A stain is forming on a polyester textile when the water invades from the left reservoir. Images at the right show the accumulated dye on the contour is washed away due to its low colorfastness (D_f).

liquids in different colors. This example shows two dye diffusion actions, diffusion with liquid and diffusion in the wetted region. Because the two liquids are soluble, the red and blue dye particles mix together at the wetted contact regions where a transitive color appears. Fig. 14 shows the application of stain simulation in a scene. Here the stain liquid is red wine. As is known, wines have low dye saturation of red pigment particle. The tablecloth is made of cotton. The colorful pigment particles stuck in the cotton fiber while the water (about 80 percent) and alcohol spread much wider. This is clearly generated and shown in the middle image.
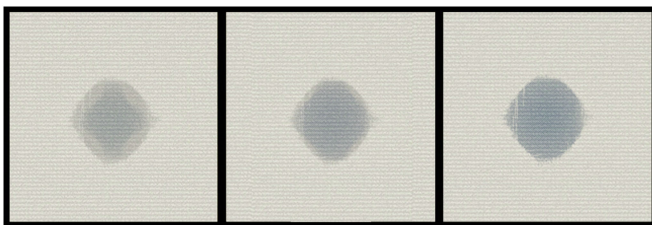

Fig. 17. Stains of different dye saturations on cotton. From left to right, the dye saturations are 0.2, 0.6 and 1.0 respectively.
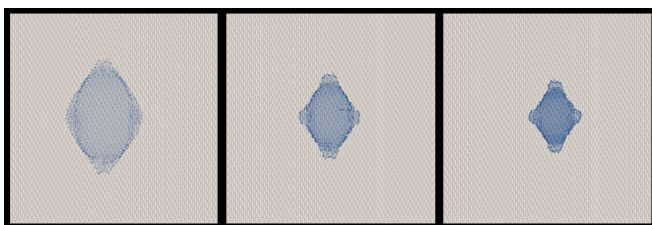

Fig. 18. Different evaporation ratios result in evident difference of stains on a polyester. The evaporation ratios from left to right are 1.0, 2.0, 3.0 respectively.

In the textile industry, some dyeing technics create desirable patterns by changing the colorfastness of the given fabric. The traditional Chinese wax painting is a good example. The basic idea is to utilize the hydrophobicity of wax to modify the local colorfastness such that the given pattern will absorb less pigment. After dyeing, the pigment on the waxing area will be washed away and the beautiful pattern will appear. This process can also be simulated by the proposed technique, as is shown in Fig. 15.

The final result in Fig. 16 shows the wash away effect, where a stain is forming on a fabric when the water comes from the left invades. The dye accumulated at the contour is washed away as shown at the right side image since the colorfastness (D_f) is low for this artificial fabric.

The statistics of computation costs of the demos are given in Table 3. All test cases are run on a PC with a 2.6 GHz Intel Core i7-6700HQ CPU with 16 GB RAM.

7 CONCLUSIONS AND FUTURE WORK

In conclusion, we propose techniques to simulate stains on fabric materials. The technique is based on physical rules and tailored for computer graphics applications. The proposed TLM is essential for the simulation of many stain effects, like the wetting cases of wool, the anisotropic diffusion effect and

TABLE 3
The Computation Cost for the Demos

Test Case	Resolution	Time for 500 Iterations
Stain of Coffee	256×256	≈ 200 s
Wrong Ink	256×256	≈ 900 s
Stain of Wine	256×256	≈ 600 s
Wax Printing	512×512	$\approx 70,000$ s
Wash Away	256×256	$\approx 2,500$ s

the sawtooth edge effect of various fabrics. The process of liquid diffusion and dye diffusion is formalized and simplified for implementation. The experimental results demonstrate that the proposed technique can be used to efficiently simulate various stains we see in everyday life. Therefore our techniques could be used in various applications, such as to reinforce the realism of a character's clothes in video games or to preview the dyeing result in printing and textile industry.

The proposed solution has some limitations: First, the chemical reaction is not considered nor is the deposition of solute; Second, the simulated fabrics are in a normal state without considering the external force that changes the microcapillary structure of yarns; Third, only normal woven fabrics are considered. Stains on some textile materials, like knitwear and carpet which are unable to be discretized into yarn-cross matrix, could not be handled in our system; Finally, different liquid solvents cannot yet be manipulated simultaneously.

In future, our research will focus on the multi-stain simulation of different liquid solutions. Simulating stains on fabrics which are not made of warp and weft yarn, like knitwear, is another interesting topic.

ACKNOWLEDGMENTS

REFERENCES

[1] F. W. Sears and M. W. Zemanski, *University Physics*. 2nd ed. Boston, MA, USA: Addison Wesley, 1955.
[2] N. R. S. Hollies, M. M. Kaessinger, B. S. Watson, and H. Bogaty, "Water transport mechanism in textile materials part II: Capillary-type penetration in yarns and fabrics," *Textile Res. J.*, vol. 27, no. 1, pp. 8–13, 1957.
[3] Y.-L. Hsieh, "Liquid transport in fabric structures," *Textile Res. J.*, vol. 65, no. 5, pp. 299–307, 1995.
[4] E. W. Washburn, "The dynamics of capillary flow," *Phys. Rev.*, vol. 17, no. 3, pp. 273–283, 1921.
[5] P. Dejlová and J. Wiener, "Wicking and wetting in textiles," *AUTEX Res. J.*, vol. 3, no. 2, pp. 64–71, 2003.
[6] E. A. Wulkow, L. C. Buckles, F. W. Minor, and A. M. Schwartz, "The migration of liquids in textile assemblies: Part II: The wicking of liquids in yams," *Textile Res. J.*, vol. 29, pp. 931–939, 1959.
[7] D. Brook and A. B. Nyoni, "Wicking mechanisms in yarns-The key to fabric wicking performance," *J. Textile Inst.*, vol. 97, pp. 119–128, 2006.
[8] V. K. Kothari, A. Ghosh, A. Patnaik, and R. S. Rengasamy, "Wetting and wicking in fibrous materials," *Textile Progress*, vol. 38, pp. 1–105, 2006.
[9] Y. Zhang, H. Wang, C. Zhang, and Y. Chen, "Wicking and wetting in textiles," *J. Mater. Sci.*, vol. 42, no. 19, pp. 8035–8039, 2007.
[10] M. Takatera and C. Zhu, "Effect of fabric structure and yarn on capillary liquid flow within fabrics," *J. Fiber Bioengineering Informat.*, vol. 6, no. 2, pp. 205–215, 2013.
[11] N. Pan, D. Lukas, and E. Glazyrina, "Computer simulation of liquid wetting dynamics in fiber structures using the ising model," *J. Textile Inst.*, vol. 88, pp. 149–161, 1997.
[12] M. Huber, S. Pabst, and W. Stra/betaer, "Wet cloth simulation," in *Proc. ACM SIGGRAPH Posters*, 2011, Art. no. 10.
[13] R. Parachuru and S. Mhetre, "The effect of fabric structure and yarn-to-yarn liquid migration on liquid transport in fabrics," *J. Textile Inst.*, vol. 101, 2010, Art. no. 931.
[14] T. Liu, K.-F. Choi, and Y. Li, "Wicking in twisted yarns," *J. Colloid Interface Sci.*, vol. 318, no. 1, pp. 134–139, 2008.
[15] S. K. Mhetre, "Effect of fabric structure on liquid transport, ink jet drop spreading and printing quality," Ph.D. dissertation, Georgia Inst. Technol., Atlanta, GA, 2009.
[16] A. H. Basori, M. Alkawaz, T. Saba, and A. Rehman, "An overview of interactive wet cloth simulation in virtual reality and serious games," *Comput. Methods Biomechanics Biomed. Eng. Imag. Vis.*, vol. 6, pp. 1–8, 2018.
[17] Y. J. Chen, N. Thalmann, and B. Allen, "Physical simulation of wet clothing for virtual human," *Vis. Comput.*, vol. 28, pp. 765–774, Jun. 2012.
[18] W. Yamada, T. Watanabe, M. Kakimoto, K. Mikami, and R. Takeuchi, "Reproduction of the behavior of the wet cloths taking the atmospheric pressure into account," in *Proc. ACM SIGGRAPH Posters*, 2013, Art. no. 12.
[19] R. Wang and S. Xiao, "Motion simulation of wet cloth on contact surface considering air effects and humidity," in *Proc. 15th ACM SIGGRAPH Conf. Virtual-Reality Continuum Appl. Ind.-Volume 1*, 2016, pp. 89–95.
[20] J. Dorsey, H. Rushmeier, and F. X. Sillion, *Digital Modeling of Material Appearance*. Burlington, MA, USA: Morgan Kaufmann, 2007.
[21] H. W. Jensen, J. Legakis, and J. Dorsey, "Rendering of wet materials," in *Proc. Rendering Techn.*, 1999, pp. 273–282.
[22] J. Dorsey, A. Edelman, H. W. Jensen, J. Legakis, and H. K. Pedersen, "Modeling and rendering of weathered stone," in *Proc. 26th Annu. Conf. Comput. Graph. Interactive Techn.*, 1999, pp. 225–234.
[23] J. Lu, A. S. Georghiades, H. Rushmeier, J. Dorsey, and C. Xu, "Synthesis of material drying history: Phenomenon modeling, transferring and rendering," in *Proc. Eurographics Workshop Natural Phenom.*, 2005, pp. 7–16.
[24] N. S.-H. Chu and C.-L. Tai, "MoXi: Real-time ink dispersion in absorbent paper," *ACM Trans. Graph.*, vol. 24, no. 3, pp. 504–511, Jul. 2005.
[25] J. Gu, C.-I. Tu, R. Ramamoorthi, P. Belhumeur, W. Matusik, and S. Nayar, "Time-varying surface appearance: Acquisition, modeling and rendering," *ACM Trans. Graph.*, vol. 25, no. 3, pp. 762–771, Jul. 2006.
[26] J. Lu, A. S. Georghiades, A. Glaser, H. Wu, L. Yi Wei, B. Guo, J. Dorsey, and H. Rushmeier, "Context-aware textures," *ACM Trans. Graph.*, vol. 26, no. 1Jan. 2007, Art. no. 3.
[27] Y. Morimoto, R. Tsuruno, and K. Tomimatsu, "Liquid penetration modeling for cloth dyeing," in *Proc. 3rd Eurographics Conf. Comput. Aesthetics Graph. Vis. Imag.*, 2007, pp. 97–104.
[28] Y. Morimoto, M. Tanaka, R. Tsuruno, and K. Tomimatsu, "Visualization of dyeing based on diffusion and adsorption theories," in *Proc. 15th Pacific Conf. Comput. Graph. Appl.*, 2007, pp. 57–64.
[29] T. Lenaerts, B. Adams, and P. Dutré, "Porous flow in particle-based fluid simulations," *ACM Trans. Graph.*, vol. 27, no. 3, pp. 49:1–49:8, Aug. 2008.
[30] C. J. Curtis, S. E. Anderson, J. E. Seims, K. W. Fleischer, and D. H. Salesin, "Computer-generated watercolor," in *Proc. 24th Annu. Conf. Comput. Graph. Interactive Techn.*, 1997, pp. 421–430.
[31] S. Xu, H. Tan, X. Jiao, F. C. Lau, and Y. Pan, "A generic pigment model for digital painting," *Comput. Graph. Forum*, vol. 26, no. 3, pp. 609–618, 2007.
[32] C.-M. Wang and R.-J. Wang, "Image-based color ink diffusion rendering," *IEEE Trans. Vis. Comput. Graph.*, vol. 13, no. 2, pp. 235–246, Mar./Apr. 2007.
[33] N. Adabala, N. Magnenat-Thalmann, and G. Fei, "Real-time rendering of woven clothes," in *Proc. ACM Symp. Virtual Reality Softw. Technol.*, 2003, pp. 41–47.
[34] K. Daubert, H. P. A. Lensch, W. Heidrich, and H.-P. Seidel, "Efficient cloth modeling and rendering," in *Proc. 12th Eurographics Conf. Rendering*, 2001, pp. 63–70.
[35] E. Gröller, R. T. Rau, and W. Straβer, "Modeling and visualization of knitwear," *IEEE Trans. Vis. Comput. Graph.*, vol. 1, no. 4, pp. 302–310, Dec. 1995.
[36] Y.-Q. Xu, Y. Chen, S. Lin, H. Zhong, E. Wu, B. Guo, and H.-Y. Shum, "Photorealistic rendering of knitwear using the lumislice," in *Proc. 28th Annu. Conf. Comput. Graph. Interactive Techn.*, 2001, pp. 391–398.
[37] W. Jakob, A. Arbree, J. T. Moon, K. Bala, and S. Marschner, "A radiative transfer framework for rendering materials with anisotropic structure," *ACM Trans. Graph.*, vol. 29, no. 4, pp. 53:1–53:13, Jul. 2010.
[38] S. Zhao, W. Jakob, S. Marschner, and K. Bala, "Structure-aware synthesis for predictive woven fabric appearance," *ACM Trans. Graph.*, vol. 31, no. 4, pp. 75:1–75:10, Jul. 2012.

Yi Zheng received the BSc degree in animation technology and the MSc degree in art of design from Communication University of China, in 2006 and 2009, respectively. He is currently working towards the PhD degree in computer science in the Institute of Software, Chinese Academy of Sciences. His research interests include computer graphics and physically based rendering.
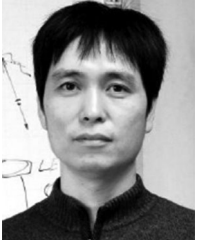
Yanyun Chen received the BSc and MSc degrees from the China University of Mining and Technology, in 1993 and 1996, respectively, and the PhD degree in computer science from the Institute of Software, Chinese Academy of Sciences, in 2000. He worked for Microsoft Research Asia and Autodesk China Research and Development Center. He became a research professor with the State Key Laboratory of Computer Science, Institute of Software, Chinese Academy of Sciences since 2010. His research interests include realistic image synthesis, modeling and rendering of complex surface appearance, and virtual reality.

Guangzheng Fei received the BSc degree from Anhui Normal University, in 1994 and MSc degree from the HeFei University of Technology, in 1997, and the PhD degree from the Institute of Software, Chinese Academy of Sciences, in 2001. He worked in Microsoft Research Asia as a visiting student and then as a postdoc in MIRALab of University of Geneva. He became a full professor with the School of Animation and Digital Arts of Communication University of China, in 2009. He worked as a visiting scholar, in 2008 and 2009, in University of Ottawa. His research interests include sketch based modeling and animation, non-photorealistic rendering, and texture synthesis.

Julie Dorsey received the undergraduate degrees in architecture and graduate degrees in computer science from Cornell University. She is a professor of computer science with Yale University, where she teaches computer graphics. She came to Yale, in 2002 from MIT, where she held tenured appointments in both the Department of Electrical Engineering and Computer Science (EECS) and the School of Architecture. Her research interests include photorealistic image synthesis, material and texture models, and sketch-based modeling. Her current and recent professional activities include service as the editor-and-chief of the *ACM Transactions on Graphics* (2012-15) and membership on the editorial boards of foundations and trends in Computer Graphics and Vision, Computers and Graphics, and the *IEEE Transactions on Visualization and Computer Graphics*. She has received several professional awards, including MIT's Edgerton Faculty Achievement Award, a National Science Foundation Career Award, an Alfred P. Sloan Foundation Research fellowship, along with fellowships from the Whitney Humanities Center at Yale and the Radcliffe Institute at Harvard.

Enhua Wu received the BSc degree from Tsinghua University, Beijing, in 1970, and stayed in the same university for teaching until 1980. He received the PhD degree from the University of Manchester, United Kingdom, in 1984, followed by working with the State Key Laboratory of Computer Science, Institute of Software, Chinese Academy of Sciences since 1985, and at the same time invited as a full professor of University of Macau since 1997. He has been invited to chair various conferences including recently the PC chair of ACM VRST15, honorary chair of SIGGRAPH Asia16 & ACM VRCAI16, co-chair of CASA18 and ACM VRCAI18. He was the editor-in-chief of the *Chinese Journal of CAD & Graphics* between 2004-2010, and an associate editor-in-chief of the *Journal of Computer Science and Technology* since 1995. He has been also in long years until now served as an associate editor for TVC, CAVW, Visual Informatics, IJIG, IJSI. He is a member of IEEE & ACM, and a fellow of the China Computer Federation (CCF). His research interests include realistic image synthesis, physically based simulation and virtual reality.

▷ **For more information on this or any other computing topic, please visit our Digital Library at** www.computer.org/publications/dlib.